crystals

MDPI

Article

A Novel Method to Determine Deformation Strain in a High-Temperature Mushy Zone for a Typical Electrical Strip Under Twin-Roll Strip Casting

Wenli Hu [1], Yali Hou [1], Jianhui Shi [2,*], Jinhua Zhao [3,*] and Lifeng Ma [1]

[1] School of Mechanical Engineering, Taiyuan University of Science and Technology, Taiyuan 030024, China
[2] School of Mechanical and Vehicle Engineering, Linyi University, Linyi 276000, China
[3] School of Materials Science and Engineering, Taiyuan University of Science and Technology, Taiyuan 030024, China
* Correspondence: sjh051208@126.com (J.S.); jhzhao2010@163.com (J.Z.); Tel.: +86-03512161126 (J.Z.)

Abstract: An evaluation method was proposed to calculate the deformation strain of a high-temperature mushy zone (HTMZ) related to twin-roll strip casting (TSC) with regard to typical 6.5 wt.% Si electrical steel (6.5 Si steel) on the basis of the crystal—plasticity theory. The viscoplasticity self-consistent (VPSC) model was applied to calculate the evolution discipline of crystallographic orientation (CRO) for the studied 6.5 Si steel processed by different deformation strains under a deformation mode of plane strain, and the deformation strain of HTMZ for the studied 6.5 Si steel related to TSC was further estimated by comparing the CRO feature achieved by theoretical calculation and experimental characterization. Results indicate that the distribution feature of CRO obtained by theoretical calculation becomes increasingly similar to those obtained through experimental characterization with the deformation strains increasing from 0 to 1.5. The ratio between the distribution intensities corresponding to R-Cube texture, the typical rolling texture of α-fiber, and the Cube texture achieved by theoretical calculation is the closest to the value obtained by experimental characterization at deformation strain of 1.4, and the deformation strain of HTMZ for the studied 6.5 Si steel involved in TSC is determined to be ~1.4.

Keywords: 6.5 Si steel; crystallographic orientation; twin-roll strip casting

check for updates

Academic Editor: Jan Macutkevic

Received: 18 January 2025
Revised: 9 February 2025
Accepted: 10 February 2025
Published: 13 February 2025

Citation: Hu, W.; Hou, Y.; Shi, J.; Zhao, J.; Ma, L. A Novel Method to Determine Deformation Strain in a High-Temperature Mushy Zone for a Typical Electrical Strip Under Twin-Roll Strip Casting. *Crystals* **2025**, *15*, 178. https://doi.org/10.3390/cryst15020178

Copyright: © 2025 by the authors. Licensee MDPI, Basel, Switzerland. This article is an open access article distributed under the terms and conditions of the Creative Commons Attribution (CC BY) license (https://creativecommons.org/licenses/by/4.0/).

1. Introduction

Twin-roll strip casting (TSC) technology, consisting of a composite continuous casting process and rolling process, is widely applied to fabricate various kinds of alloys including structural steel and stainless steel, as well as electrical steel, and it is regarded as a promising technology characterized by environmental protection and energy saving comparable to the conventional thermo-mechanical controlled process due to the short-process design [1–4]. Since TSC is a complex coupled process involving physical metallurgical behaviors such as metal flow, solidification, and plastic deformation, cracking is prone to occur when TSC is applied to fabricate a strip, and the problem associated with surface quality control of the strip has become a predominant problem restricting the development and further industrial application of TSC.

Generally, the high-temperature zone of metals and alloys, which consists of a dual phase including the solid phase and liquid phase, is regarded as high-temperature mushy zone (HTMZ) due to weak liquidity. For the investigations of surface quality control of strip processed by TSC, the reported papers have indicated that surface roughness of

casting rolls, surface morphology of casting rolls, as well as rolling force during TSC were the predominant factors influencing the surface quality of casting strip [5–10]. Taking the rolling force into account, Buchner et al. proposed that a larger rolling force could intensify the heat transfer process between the crystallization rollers and the casting strip, inevitably leading to a strong temperature gradient, which could easily cause cracking. On the contrary, surface cracking could be lessened by reducing the rolling force during TSC [5]. Fujita Y et al. investigated the influences of roller gap and rolling force on the deformation behavior of HTMZ, and results indicated that more serious cracking was prone to occur induced by severe plastic deformation at the processing conditions of a smaller roller gap and larger rolling force [6]. To summarize, the surface quality of a casting strip could be improved by performing a roughness treatment, implementing a morphology design on the surface of the casting roller, or by coating the surface of the casting roller, and the above influencing factors could be classified as external factors. Similarly, the surface quality of a casting strip could be improved from the perspective of rolling force, and it could be classified as internal constraints. For the external influencing factors, the cracking mechanism has been fully understood and illuminated from a degree of heat transfer and solidification uniformity [7–11]. However, there are few research reports on the internal factors, such as rolling force, which has led to a lack of relevant investigations on cracking from the perspective of plastic deformation.

The practice of TSC has shown that the deformation behavior of the HTMZ was closely related to the surface quality control of the strip, and if the selection of processing parameters related to TSC was unreasonable, cracking was easily generated in the HTMZ. In accordance with the plastic deformation theory and fracture theory of metal and alloys, it could be fundamentally confirmed that cracking could occur when the stress borne by the solidified shell exceeded the allowable amount of strength and the allowable strain. Furthermore, it could be estimated that the understanding of cracking could be traced to the feature of deformation strain induced by the rolling force, and the relation between deformation strain and the cracking phenomenon could be regarded as a significant criterion to evaluate the crack sensitivity involved in TSC. While the determination of deformation strain has become a problem due to TSC being performed in HTMZ, the traditional plastic deformation theory could not be utilized. The reported research indicated that due to the presence of the liquid phase, the mechanical properties between the HTMZ and solid phase regions were absolutely different [12,13]. The conventional plastic deformation theory, including elastic–plastic deformation, rigid plastic deformation, and the viscoplastic deformation theory could only be utilized under continuous point conditions, and the fundamental mechanic laws and constitutive relations could be applied [14,15]. However, there was no ideal macroscopic plastic deformation theory applicable for the simulation and calculation of deformation behavior for the strip processed by TSC due to the continuous points being destroyed by the existence of the liquid phase in the HTMZ. For this purpose, a novel method describing the deformation behavior of the high-temperature mushy zone was proposed by our research team on the basis of the crystal–plasticity theory with respect to typical electrical steel, and the deformation mechanism of the studied metal alloy involved in TSC could be illuminated following this method [16].

Since there is no ideal research method to characterize the deformation strain of HTMZ involved in the TSC, to solve this issue we focused on the characterization of deformation strain by considering the deformation mechanism for representative electrical steel, and a novel method to evaluate the deformation strain involved in the HTMZ is proposed on the basis of crystal–plasticity theory, which is expected to provide reference for deformation strain measurement of the other metal or alloys under TSC.

2. Materials and Mathematical Model Establishment

2.1. Materials and Microstructual Characterization

In this study, typical 6.5 wt.% Si electrical steel (6.5 Si steel) with a thickness of 3 mm processed by TSC was selected as the raw experimental material, and its specific chemical composition is shown in Table 1. A TSC experiment was conducted on a twin-roll strip caster designed and developed by Northeastern University in China, and the diameter and width of casting rolls were φ 500 mm and φ 250 mm, respectively. The preheating temperature of the intermediate package was selected as 1150 °C, and the superheating melting temperature was confirmed to be 30 °C.

Table 1. Chemical composition of the investigated 6.5 Si steel (mass fraction, %).

Element	C	S	P	Si	Mn	Al	Fe
Weight percent	0.130	≤0.005	≤0.03	6.52	0.400	0.150	Ballance

Since the predominant parameters including the three-dimensional dimensions of grains, and the size ratio between transverse direction and vertical direction were needed for mathematical model establishment, the sections of the investigated 6.5 Si steel, consisting of the normal direction (ND), transverse direction (TD), and the casting direction (CD), were detected by utilizing an electron back-scattered diffraction (EBSD) technique. The average value related to the three-dimensional dimensions in regard for the investigated 6.5 Si steel obtained by TSC was analyzed and selected as the original grain size for the following model establishment. The concrete experimental process and method associated with the sampling method and EBSD detection were referred to the published paper by our research team in detail [16], and the re-construction figure of the studied 6.5 Si steel is shown in Figure 1a. In this study, a grain boundary with misorientation above 15° was regarded as a large-angle grain boundary (LAGB), and the irregular-shaped grain consisting of an LAGB was equivalent to a circle. Then, the average diameter of the circle was confirmed to be the approximate grain size (AGS). The statistics of AGS corresponding to different cross sections for the investigated 6.5 Si steel is depicted in Figure 1b. For the establishment of a mathematical model, the original ellipsoidal ratio for the investigated 6.5 Si steel should be acquired, and the average value of AGS corresponding to the sections consisting of CD and TD, TD and ND, and CD and ND were determined to be ~172.30 μm, ~163.00 μm, and ~122.40 μm, respectively, and the original ellipsoidal ratio for the investigated 6.5 Si steel was estimated to be 10:9:7, which was used for the following establishment of calculation model.

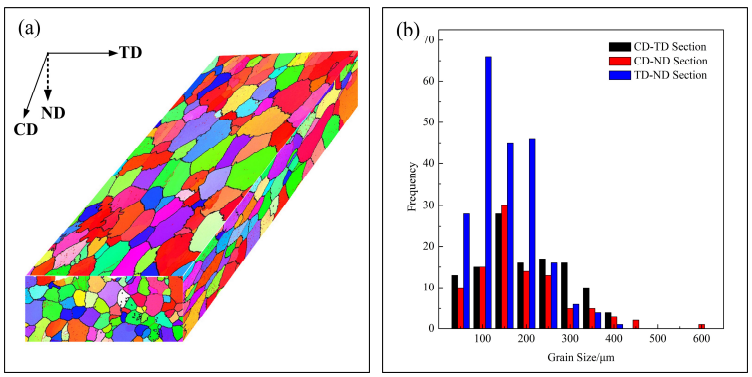

Figure 1. Crystallographic information of studied alloy obtained through EBSD analysis. (**a**) Three-dimensional morphology of grains. (**b**) Distribution of grain size corresponding to different sections for the 6.5 Si steel processed by TSC.

2.2. Mathematical Model Establishment

The viscoplasticity self-consistent (VPSC) model [17] was adopted in this study to investigate the evolution discipline of crystallographic orientation of the HTMZ for the studied 6.5 Si steel processed by TSC. For the investigated 6.5 Si steel with a body-centered crystal coordinate (BCC), the deformation mechanism dominated by dislocation slipping was predominant for the alloy verified by our previous research foundation [16], and the potential multiple slip system {110}<111>, {112}<111>, {123}<111> was confirmed to be activated. Hence, overall, 48 potential slip systems were considered in this study during the calculation process.

In addition, the significant parameters used for VPSC model establishment mainly included the parameters associated with the hardening behavior of the studied alloy. The strength of the studied alloy in the HTMZ was relatively small [12], and the strength in the HTMZ and the strength increment induced by deformation were overall ignored in present study. In order to ensure that the deformation behavior in the simulation process follows basic mechanical law, the default parameters related to the stress state of the rolling process and the original strength in reference [17] was adopted. In addition, since the high-temperature strength of the investigated 6.5 Si steel in the HTMZ was proven to be relatively small, no hardening was assumed, and all systems were assigned the same critical shear stress, and the self-hardening effect in regard for the investigated 6.5 Si steel in this study was ignored. The parameters applied for the Voce hardening model [18] were selected and shown in Table 2.

Table 2. Parameters applied for Voce hardening model for the investigated 6.5 Si steel.

Parameter Type	τ_0	τ_1	θ_0	θ_1	$h^{SS'}$
Value	2	0	1	0	0

The reported papers have proven that the texture of the casting 4.5 Si steel and 6.5 Si steel fabricated by TSC was predominantly characterized by λ-texture, and the microstructure was predominantly composed of columnar crystals characterized by <001>//ND [19–21]. During model establishment, in regard to the studied 6.5 Si steel, a 500 cube crystallographic orientation (CRO) structure with misorientation of ±15° together with 500 randomly generated CROs were utilized by referring to references [21,22], and every CRO was assigned to single grains, and the accumulated intensity of every CRO was regarded as volume fraction of different grains. Eventually, the MTEX toolbox [23,24] was utilized to display the CRO by utilizing a pole figure as shown in Figure 2. During the establishment of the VPSC model, the three-dimensional dimensions of grains for the studied strip processed by TSC was similarly regarded as the initial grain size, and the grain diameters and aspect ratio corresponding to different sections introduced in Section. 2.1 were selected as the initial parameters.

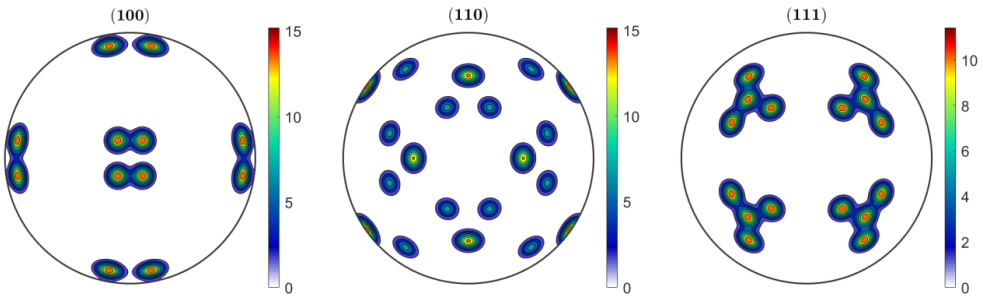

(**a**) (**b**) (**c**)

Figure 2. Constructed initial CRO for 6.5 Si steel before TSC treatment expressed by utilizing a pole figure. (**a**) (100) pole figure. (**b**) (110) pole figure. (**c**) (111) pole figure.

3. Results and Discussion

Figure 3 shows the CRO information of the investigated 6.5 Si steel processed through TSC corresponding to the section composed of CD and TD. The micro-crystallographic orientation and grain shape are depicted by utilizing the orientation-mapped figure and LAGB-mapped figure as shown in Figure 3a, and the CRO is expressed by utilizing the orientation distribution function graph (ODF) as shown in Figure 3b. In accordance with the characterization results, it could be easily found that the CRO of the investigated 6.5 Si steel obtained through TSC is mainly composed of the λ-fiber, which indicates that a large volume fraction of the (001) crystal plane involved in the TSC-processed steel is parallel to the rolling section composed of CD and TD. The texture components are predominantly composed of Cube and R-Cube. To make the texture component more easily distinguishable, the R-Cube component is further divided into R-Cube1 (phi1 = 0°, phi = 0°, phi2 = 45°) and R-Cube2 (phi1 = 90°, phi = 0°, phi2 = 45°), and the distribution intensities of R-Cube1, Cube, and R-Cube2 are determined to be 4, 5, and 5, respectively. In addition, some typical rolling texture distributed on the α-fiber (⟨110⟩//RD or CD) could also be found on the ODF, and the distribution intensity of $\{112\} < 110 >$ is detected to be 2. The CRO of the investigated 6.5 Si steel processed through TSC could be taken as a reference to explore the deformation mechanism in the following section.

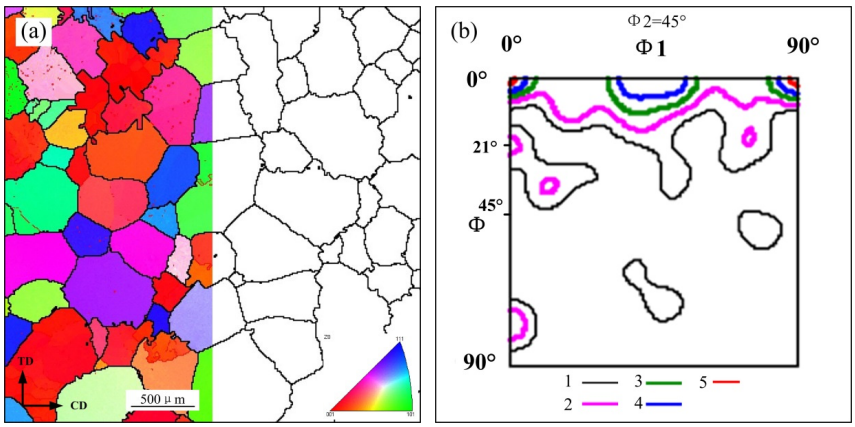

Figure 3. Crystallographic orientation feature of the investigated 6.5 Si steel. (**a**) Orientation and grain boundary distribution graph. (**b**) ODF (phi2 = 45°).

In accordance with the calculation results reported by our research team [15], the transformation rate from the initial CRO to the actual CRO achieved through EBSD detection was the fastest as comparing to the other single or multiple slip systems when the multiple slip system of {110}<111>, {112}<111>, {123}<111> was activated with respect to 6.5 Si steel. Hence, the multiple slip system of {110}<111>, {112}<111>, {123}<111> is adopted to estimate the deformation strain involved in the TSC, considering the crystal–plasticity theory. In the present study, the evolution feature of the CRO is utilized to estimate the deformation strain involved in the plastic deformation process in the HTMZ. Figure 4 shows the variation discipline of the CRO with an increasing deformation amount for the studied 6.5 Si steel under activation of the {110}<111>, {112}<111>, {123}<111> multiple slip system. It was identified that the initial texture component of the investigated steel is predominantly composed of a Cube texture before deformation, as shown in Figure 4a, and the maximum distribution intensity is determined to be ~12. With the increase in deformation amount, the distribution intensity of the Cube texture is gradually decreased, and the distribution intensities of R-Cube1 and R-Cube2 are both obviously increased, as shown in Figure 4b,c. With the deformation strain increased to 1.1, the distribution intensity corresponding to the R-Cube texture is evidently increased, with maximum intensity of 10, and the max distribution intensity corresponding to R-Cube is

increased to 11 at the deformation strain of 1.5, accompanied by the max distribution intensity corresponding to Cube decreasing to 10. In addition, the distribution intensity corresponding to the typical texture distributed on the α-fiber and γ-fiber are obviously increased, with the deformation strain increased from 0.3 to 1.5, as shown in Figure 4b–e. Generally, the α-fiber and γ-fiber are the typical oriented aggregation area of the BCC metal in the ODF figure, and they are usually induced by plastic deformation [25]. The λ-fiber is the typical oriented aggregation area of the BCC metal in the ODF figure, which is mainly attributed to the solidification process [26]. In this study, the γ and α fibers are strengthened with increasing deformation, indicating that the deformation process plays a certain role during the TSC process in regard to the studied 6.5 Si steel due to the TSC process being a coupling process of solidification and deformation. However, the influence of deformation on the formation of the CRO feature for the investigated 6.5 Si steel is limited due to the maximum of intensity corresponding to the typical texture of {111}< $\overline{1}$23> only reaching up to 2 at the deformation strain of 1.5, as shown in Figure 4e. Hence, it could be deduced that the evolution of CRO for the investigated 6.5 Si steel under TSC follows the discipline: the initial texture of Cube derived from solidification is inclined to transform into the R-Cube texture with the increase in deformation strain under the load of plane strain deformation. At the same time, some grains with a random CRO are inclined to transform into the {111}< $\overline{1}$23> texture distributed on the γ-fiber under the application of plane strain deformation.

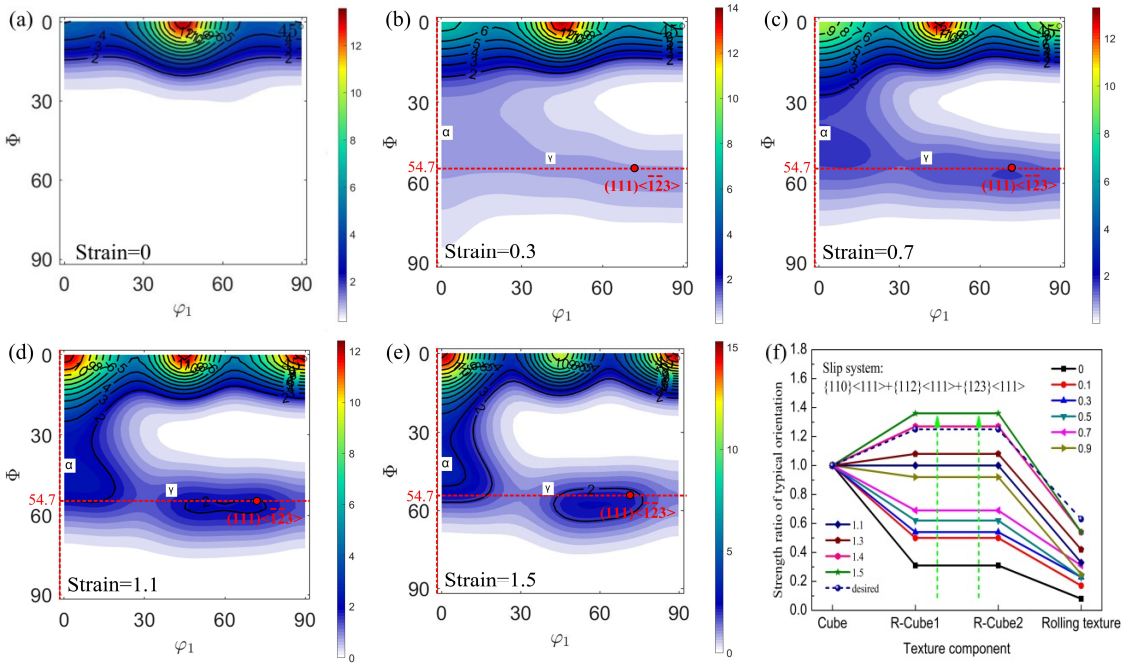

Figure 4. Orientation evolution of {001} crystallographic orientation. (**a**) 0; (**b**) 0.3; (**c**) 0.7; (**d**) 1.1; (**e**) 1.5. (**f**) Variation trends of texture features.

To further describe the distribution feature of CRO for the studied 6.5 Si steel, the relative ratio between the typical texture components of Cube, R-Cube1, and R-Cube2, as well as the rolling texture of the α-fiber is utilized as an indicator. Figure 4f gives the varying discipline of the relative ratio distribution feature corresponding to different deformation strains considering from the activation of the multiple slip system {110}<111>, {112}<111>, {123}<111>, and it could be seen that the distribution feature of the strength ratio of a typical CRO gradually approached the desired distribution feature, with the deformation strain increasing from 0.1 to 1.3. With the deformation strain increased to 1.4, the calculated distribution feature of a typical CRO almost overlapped with the actual desired feature, which indicates that the texture feature is equal to the feature under an applied deformation

strain of 1.4. Consequently, it could be determined that the deformation strain is estimated to be 1.4 by comparing the coincidence of the CRO feature for the investigated 6.5 Si steel processed by TSC.

To verify rationality of the activated slip system, the average number of active systems (AVACS) inside a single grain was estimated, and the relative activity induced by different slip systems was also calculated. Figure 5a shows the distribution feature of an average number of active systems induced by the multiple slip system of {110}<111>, {112}<111>, {123}<111> as a function of strain, and it could be determined that the AVACS inside a single grain is distributed in the value range of 10.2~10.8, which is satisfied by the Sachs theory, implying the rationality of the activated slip system. Figure 5b further gives the distribution feature of relative activity induced by different slip systems as a function of strain, and it could be determined that the relative activitities induced by slip system of {110}<111>, {112}<111>, and {123}<111> are determined to be 0.35, 0.19, and 0.46, respectively, indicating that the slip systems of {110}<111> and {123}<111> are predominant during deformation in the HTMZ for the studied 6.5 Si steel.

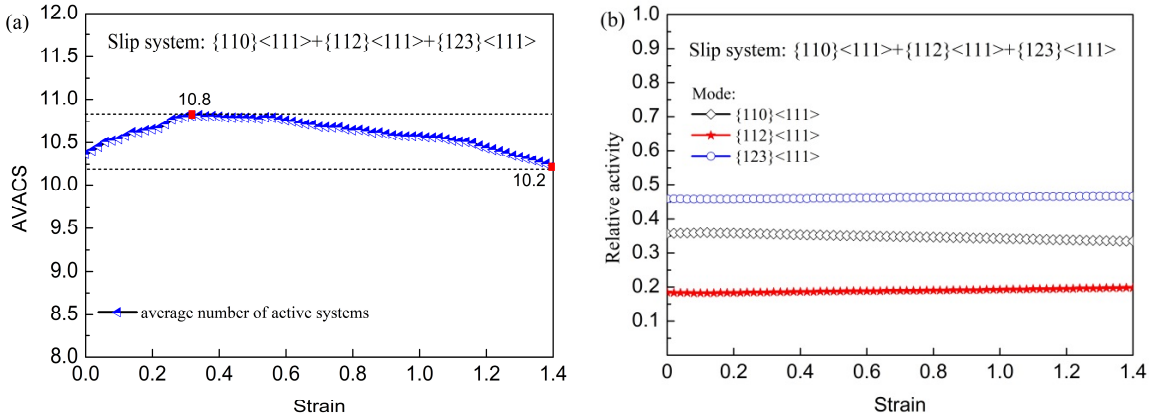

Figure 5. The calculated results associated with the deformation mechanism of the studied alloy. (**a**) Average number of active systems. (**b**) Relative activity induced by different slip systems considering the multiple slip system of {110}<111>, {112}<111>, {123}<111>.

To summarize, the VPSC model applied in this study has offered a method to estimate the evolution discipline of crystallographic orientation in regard to the 6.5 Si steel under different deformation processes, and the variation discipline of the CRO for the studied alloy was calculated and analyzed on the basis of the VPSC model, considering the initial crystallographic orientation feature, physical properties, and hardening parameters of the studied 6.5 Si steel. The deformation strain involved in the HTMZ under TSC in regard to the 6.5 Si steel was further determined by comparing the texture features achieved through theoretical calculation and experiments, which could be regarded as reference for strain measurement and the estimation of the other semi-solid deformation process.

4. Conclusions

(a) A novel method to evaluate the deformation strain involved in the HTMZ under TSC is proposed on the basis of the crystal–plasticity theory. The deformation strain of the investigated 6.5 Si steel during TSC was determined to be 1.4 by comparing the distribution feature of the CRO between the theoretical calculation and experimental characterization.

(b) The average number of active systems inside a single grain was distributed in the value range of 10.2~10.8 under the activation of a multiple slip system of {110}<111>, {112}<111>, {123}<111>, and the relative activities induced by slip system

of {110}<111>, {112}<111>, and {123}<111> were determined to be 0.35, 0.19, and 0.46, respectively.

Author Contributions: Conceptualization, L.M.; methodology, J.Z. and J.S.; validation, L.M.; investigation, W.H. and Y.H.; data curation, W.H.; writing—original draft preparation, Y.H.; writing—review and editing, W.H.; visualization, W.H.; supervision, J.Z. and J.S.; funding acquisition, W.H. All authors have read and agreed to the published version of the manuscript.

Funding: This research was funded by "Taiyuan University of Science and Technology Scientific Research Initial Funding (No. 20232023)", "Scientific and Technological Innovation Programs of Higher Education Institutions in Shanxi (No. 2022L290)", and "Applied Basic Research Program in Shanxi, China (No. 202203021212309)".

Data Availability Statement: The dataset is available upon request from the authors.

Conflicts of Interest: The authors declare no conflicts of interest.

References

1. Saini, D.K.; Jha, P.K. A hybrid approach towards evaluation of average heat transfer coefficient in twin-roll strip casting mold. *Therm. Sci. Eng. Prog.* **2024**, *49*, 102472. [CrossRef]
2. Song, H.; Wang, G.; Liu, H. Effect of cold rolling on microstructure and texture evolution in strip casting Fe-36%Ni invar alloy foil. *J. Alloys Compd.* **2021**, *888*, 161519. [CrossRef]
3. Liu, H.; Li, H.; Schneider, J.; Liu, Y.; Wang, G. Effects of coiling temperature after hot rolling on microstructure, texture, and magnetic properties of non-oriented electrical steel in strip casting processing route. *Steel Res. Int.* **2016**, *87*, 1256–1263. [CrossRef]
4. Chandramohan, D.L.; Roy, K.; Ananthi, G.B.G.; Fang, Z.; Lim, J.B.P. Structural behaivor and capacity of cold-formed steel channel sections with elongated edge-stiffened and unstiffened web holes under compression. *J. Constr. Steel Res.* **2024**, *218*, 108681. [CrossRef]
5. Buchner, A.R.; Zimmermann, H. Cracking phenomena in twin roll strip casting of steel. *Steel Res. Int.* **2002**, *73*, 327–331. [CrossRef]
6. Fujita, Y.; Sato, H.; Kitagawa, T.; Nishioka, S.; Tsuchida, Y.; Ozek, A. Solidification and roll-bonding of shells in twin-roll casting process. *ISIJ Int.* **1989**, *29*, 495–502. [CrossRef]
7. Choo, D.K.; Lee, S.; Moon, H.K.; Kang, T. Analysis and prevention of cracking during strip casting of AISI 304 stainless steel. *Metall. Mater. Trans. A* **2001**, *32A*, 2249–2258. [CrossRef]
8. Yukumoto, M.; Yamane, H. Prevention techniques of roll surface crack in twin-roll caster. *ISIJ Int.* **1996**, *4*, 26–31.
9. Sanz, A. Tribological behavior of coatings for continuous casting of steel. *Surf. Coat. Technol.* **2001**, *146–147*, 55–64. [CrossRef]
10. Li, B.Q. Producing thin strips by twin roll casting part i process aspects and quality issues. *J. Mater. Sci.* **1995**, *47*, 29–33. [CrossRef]
11. Gurupatham, B.G.A.; Roy, K.; Lim, J.B.P. Effect of stiffeners on the axial strength of face-to-face unequal-angle cold-formed steel columns. *Buildings* **2025**, *15*, 88.
12. Hu, W.L.; Zhang, Y.X.; Yuan, G.; Zhang, X.M.; Zhao, J.H.; Wang, G.D. Comparison of cracking sensitivity between high-permeability 1.5wt% Si steel and 6.5 wt% Si steel in mushy zone. *J. Magn. Magn. Mater.* **2020**, *510*, 166927.
13. Seol, D.J.; Won, Y.M.; Oh, K.H.; Shin, Y.C.; Yim, C.H. Mechanical behavior of carbon steels in the temperature range of mushy zone. *ISIJ Int.* **2000**, *40*, 356–363. [CrossRef]
14. Liu, H.W. *Mechanics of Materials*; Higher Education Press: Beijing, China, 2017.
15. Wang, Z.Q.; Duan, Z.P. *Micromechanics of Plasticity*; Science Press, China: Beijing, China, 1995.
16. Hu, W.L.; Zhang, Y.X.; Yuan, G.; Zhang, X.M.; Zhao, J.H.; Wang, G.D. Applying crystallographic orientation analysis for exploring deformation mechanism of 6.5 wt.% Si electrical strip during twin-roll thin strip casting process. *J. Mater. Res. Technol.* **2021**, *13*, 1980–1991.
17. Tome, C.N.; Lebensohn, R.A. *Manual for Code Visco-Plastic Self-Consistent (VPSC) (Version 7d)*; Los Alamos National Laboratory: Los Alamos, NM, USA, 2012.
18. Tome, C.N.; Canova, G.R.; Kocks, U.F.; Christodoulou, N.; Jonas, J.J. The relation between macroscopic and microscopic strain hardening in FCC polycrystals. *Acta Metall.* **1984**, *32*, 1637–1653.
19. Li, H.Z.; Liu, H.T.; Liu, Z.Y.; Lu, H.H.; Song, H.Y.; Wang, G.D. Characterization of microstructure, texture and magnetic properties in twin-roll casting high silicon non-oriented elecrical steel. *Mater. Charact.* **2014**, *88*, 1–6.
20. Park, J.Y.; Oh, K.H.; Ra, H.Y. The effect of superheating on texture and microstructure of Fe-4.5wt% Si strip by Twin-roll strip casting. *ISIJ Int.* **2001**, *41*, 70–75.
21. Liang, R.; Yang, P.; Mao, W. Retaining {100} texture from initial columnar grains in 6.5wt% Si electrical steels. *J. Magn. Magn. Mater.* **2017**, *441*, 511–516.

22. Wang, F.; Liu, Z.F.; Hu, W.L.; Zhao, J.H.; He, W.W.; Hou, H. Understanding and exploring anisotropy mechanism of mechanical properties for ferrous alloy under different cooling paths. *J. Mater. Res. Technol.* **2024**, *32*, 261–272.
23. Hielscher, R.; Schaeben, H. A novel pole figure inversion method: Specification of the MTEX algorithm. *J. Appl. Crystallogr.* **2008**, *41*, 1024–1037.
24. Bachmann, F.; Hielscher, R.; Schaeben, H. Grain detection from 2d and 3d EBSD data specification of the MTEX algorithm. *Ultramicroscopy.* **2011**, *111*, 1720–1733. [PubMed]
25. Jonas, J.J.; Haldar, A.; Suwas, S.; Bhattacharjee, D. (Eds.) *Microstructure and Texture in Steels and Other Materials*; Springer: London, UK, 2008; pp. 3–17.
26. Li, H.Z.; Liu, H.T.; Liu, Z.Y.; Wang, G.D. Effects of warm temper rolling on microstructure, texture and magnetic properties of strip-casting 6.5 wt% Si electrical steel. *J. Magn. Magn. Mater.* **2014**, *370*, 6–12.

Disclaimer/Publisher's Note: The statements, opinions and data contained in all publications are solely those of the individual author(s) and contributor(s) and not of MDPI and/or the editor(s). MDPI and/or the editor(s) disclaim responsibility for any injury to people or property resulting from any ideas, methods, instructions or products referred to in the content.